Water Resources Research Institute
of The University of North Carolina

Report No. 429

IMPACT OF SEDIMENT PROCESSES ON WATER QUALITY IN THE NEUSE RIVER ESTUARY

By
Yonghong Nie, Marc J. Alperin

Department of Marine Sciences
University of North Carolina at Chapel Hill
Chapel Hill, NC 27599-3300

UNC-WRRI-429

The research on which this report is based was supported by funds provided by the North Carolina General Assembly through the North Carolina Department of Environment and Natural Resources.

This report fulfills the requirements for a project completion report of the Water Resources Research Institute of The University of North Carolina. The authors are solely responsible for the content and completeness of the report.

WRRI Project No. 70176
June 2008

ACKNOWLEDGMENTS

This report benefited from the assistance of many people. Brent Ream, John Fear, Dan Albert, and Howard Mendlovitz assisted with field and laboratory work used to acquire the data for model calibration. Sara Haines and Marcus Cox helped with the computer software used in the model. Funding for this project was provided by the Water Resources Research Institute of the University of North Carolina.

ABSTRACT

A primary control on the estuarine nitrogen cycle involves interactions between the water column and the sediments. These interactions are particularly important in shallow, slow-flowing estuaries like the Neuse where a large portion of the organic matter produced in the water column reaches the sediment surface. Although time delays between deposition and remineralization allow sediments to retain nitrogen over seasonal and annual time scales, most detrital nitrogen that enters the sediment is ultimately remineralized. The product of organic nitrogen remineralization—primarily NH_4^+—faces two possible fates: it may diffuse to the overlying water, where it can stimulate algal production, or it may be converted to NO_3^- by aerobic nitrifying bacteria. The production of NO_3^- (nitrification) is of particular interest because it can stimulate denitrification, an anaerobic process whereby NO_3^- is converted to N_2 and rendered unavailable to most algae. Thus, the flux of NH_4^+ and NO_3^- across the sediment-water interface is controlled by a delicate balance between ammonium production, nitrification, and denitrification. These three processes have the properties of a highly nonlinear system: they are tightly coupled and partly regulated by O_2 concentrations that vary in space and time. As a result, the contribution of bottom sediments to nitrogen loading in the estuary is difficult to quantify and even more difficult to predict. In this report, we develop, calibrate, and apply a multi-component diagenetic model that simulates sediment process and provides a quantitative estimate of the benthic flux of NH_4^+, NO_3^-, and O_2. We use this model to predict how these fluxes may be impacted by (1) a reduction on nitrogen loading to the estuary, (2) changes in hypoxia/anoxia in the overlying water, and (3) variable bottom current.

TABLE OF CONTENTS

LIST OF FIGURES

LIST OF TABLES

SUMMARY AND CONCLUSIONS

Sediment-water column interactions in the Neuse River estuary are highly nonlinear and characterized by numerous positive and negative feedbacks between master variables (such as nitrogen loading and sediment organic matter deposition) and response variables (such as internal cycling of nitrogen and total oxygen demand). The sediment diagenesis model presented here is a tool for making quantitative predictions of how the sediment system, and resulting benthic fluxes, respond to various scenarios involving changes in the master variables. The most important results from the sediment model are as follows:

1. Sediment oxygen demand responds slowly to a sudden reduction sedimentary organic matter deposition. This is because the sediments contain a large repository of reactive organic that serves as a time-release source of oxygen demand. Following a reduction of organic matter deposition, it will take 15 years for the sediment oxygen demand to decrease to 50% of its steady-state value.

2. The reduction in the steady-state benthic oxygen flux is not proportionate to the reduction in SOM deposition. For example, a 30% reduction in SOM flux translates to only a 20% reduction in benthic oxygen flux.

3. The reduction in the steady-state benthic ammonium flux is more than proportionate to the reduction in SOM deposition. For example, a 30% reduction in SOM flux translates to a 73% reduction in benthic ammonium flux.

4. Reduced SOM deposition will shift the nitrogen species released from the sediments in favor of more nitrate and less ammonium.

5. Episodic hypoxia and anoxia in the bottom water result in elevated benthic fluxes of reactive nitrogen to the water column.

6. Variations in bottom current introduce internal variability in sediment-water column exchange processes. The benthic oxygen flux increases markedly with bottom current while denitrification slightly reduced at higher bottom water velocities. The benthic ammonium flux is controlled by processes well below the diffusive boundary layer and is little affected by bottom current.

RECOMMENDATIONS

1. Exchange of carbon, nitrogen, and oxygen between the water column and the sediment must be an integral part of any estuarine water quality model.

2. The “lifetime” of sedimentary organic matter is the key variable for defining the rate at which the estuary will respond to changes in nitrogen loading. Hence, more work is needed to better constrain this variable in the Neuse River estuary.

3. The response time of the Neuse River estuary to a reduction in nitrogen loading is on the order of decades. Hence, long-term records of key environmental parameters (e.g., duration and extent of bottom water hypoxia/anoxia) are needed to establish the extent to which the estuarine system is approaching its “background” condition.

INTRODUCTION

In this report, we discuss the development and application of a sediment process model that simulates and predicts the impact of sediment processes on water quality in the Neuse River estuary. Emphasis has been placed on capturing the details of the sediment-water interface—in particular, the diffusive boundary layer—in order to accurately simulate the impact of bottom water currents and concentrations on sediment processes and benthic fluxes.

This sediment model is applied in Neuse River estuary in North Carolina, USA (Figure 1). The Neuse River estuary shows many symptoms of an over-productive estuary: algal blooms, bottom water anoxia, and fish kills. Like most coastal ecosystems, primary production in the Neuse River estuary is generally limited by nitrogen (Paerl 1987; Paerl et al. 1990; Rudek et al. 1991). Anthropogenic nitrogen loading to the Neuse River basin has more than doubled since 1960 due to rapid growth in population and intensive agriculture (Stanley 1997). Although the link between increased watershed nitrogen loading and phytoplankton biomass within the estuary is difficult to establish (e.g., Stanley et al. 2000; Stow et al. 2001), there is a widespread perception that impaired water quality within the Neuse River estuary is related to cultural eutrophication.

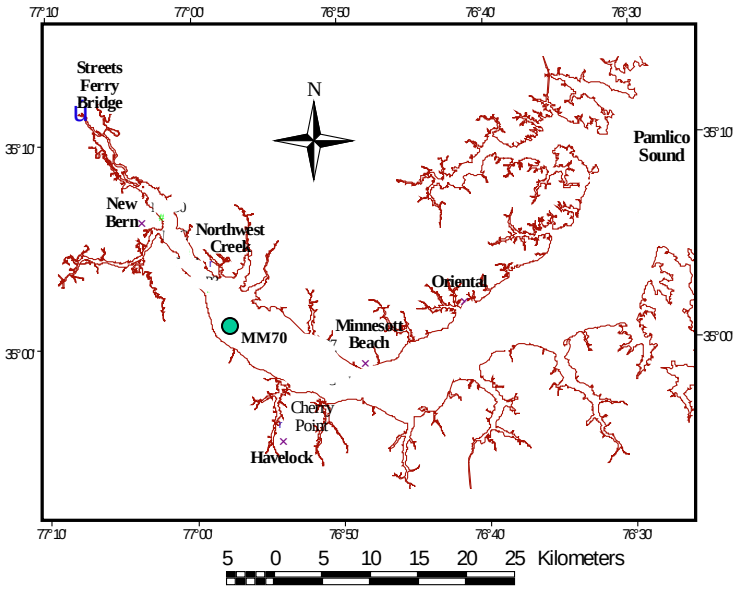

Figure 1. Map of the Neuse River estuary showing station MM70.

In an attempt to reduce primary production in Neuse River estuary, the North Carolina General Assembly has enacted legislation requiring a 30% reduction in nitrogen loading. While it is generally agreed that reduced nitrogen input will result in lower productivity, the long-term impact and the estuarine response time to nitrogen reduction are difficult to predict. This is because nitrogen is recycled through numerous biogeochemical compartments within the estuary before ultimately being removed by export, denitrification, or burial.

One of the primary controls on the estuarine nitrogen cycle is interaction between the water column and the sediments. This interaction is particularly important in shallow, slow-flowing estuaries like the Neuse where a large portion of the organic matter produced in the water column reaches the sediment surface (Suess 1980; Nixon 1981). In these systems, the benthic ammonium flux is an important, time-release source of recycled nitrogen to the water column. On the other hand, sediment denitrification is an important process for removing excess nitrogen from the estuary. Sediment-water column interactions also provide important controls on bottom-water hypoxia. Sediments in the Neuse River estuary are rich in organic matter and play an important role in the estuarine oxygen budget.

The sediment process model provides a tool for making quantitative predictions as to how sediment oxygen demand, benthic ammonium flux, and denitrification rates will respond to reduced nitrogen loading to coastal environment.

SEDIMENT PROCESS MODEL

DIFFUSIVE BOUNDARY LAYER

Since the model focuses explicitly on sediment-water column interactions, we need to simulate the fluid dynamics in the vicinity of the sediment-water interface. D_E is the eddy diffusivity created by turbulence in the water column. The height dependence of D_E is given as (Van Driest equation, Boudreau 2001):

$$D_E = \frac{\nu}{2}\left(\left\{1 + 4\kappa^2 Z^2\left[1 - \exp\left(-\frac{Z}{26}\right)\right]^2\right\}^{1/2} - 1\right), \quad (1)$$

where ν is kinematic viscosity of water, κ is Von Karman's constant (0.4), and Z is dimensionless height, ($Z = (xU^*)/\nu$). The shear velocity (U^*) is calculated according to Sternberg (1968) and Hickey et al. (1986):

$$Cd = 10^{-3}(2.33 - 0.0526U_{100} + 0.000365U_{100}^2), \quad (2)$$

$$U^* = (Cd)^{1/2}U_{100}. \quad (3)$$

where Cd is the drag coefficient (unitless), and U_{100} is current velocity 1-meter above the sediment surface. The thickness of diffusive sublayer (δ_D) is calculated as:

$$Sc = \nu / D_0, \quad (4)$$

$$\delta_D = \frac{D_0}{0.078(Sc)^{-2/3}U^*}, \quad (5)$$

where Sc is the Schmitt number (Opdyke et al. 1987; Santschi et al. 1991; Boudreau 1997), and D_0 is the molecular diffusion coefficient.

SEDIMENT PROCESSES

The sediment model is based on a set of coupled, nonlinear differential equations that describe physical transport within the benthic boundary layer and surficial sediments, and chemical and biological processes associated with sedimentary organic matter (SOM) degradation (Rabouille and Gaillard 1991; Soetaert et al. 1996a; Boudreau 1997). The primary reactions involve microbially-mediated organic matter remineralization, including aerobic respiration, denitrification, sulfate reduction, and methanogenesis. The secondary reactions involve oxidation of the reduced end-products from the primary biogeochemical reactions and include nitrification, methane oxidation, and Fe^{2+}/sulfide oxidation. The primary and secondary reactions included in the model are summarized in the Appendix.

Sedimentary organic matter (SOM) is the master variable for the sediment model. We use the standard "multi-G" convention for parameterizing the SOM pool (e.g., Westrich and Berner

1984; Soetaert et al. 1996a, 1996b). SOM is represented by two degradable fractions (SOM_1 and SOM_2) with different first-order rate constants, and one refractory fraction (SOM_3). Depth distributions of SOM pools are described by the following diagenetic equations:

$$\frac{\partial\left((1-\phi)\rho[SOM_1]\right)}{\partial t} = \frac{\partial\{(1-\phi)\rho D_B \frac{\partial[SOM_1]}{\partial x}\}}{\partial x} - \frac{\partial\{(1-\phi)\rho\omega[SOM_1]\}}{\partial x} - (1-\phi)\rho k_1[SOM_1] \quad (6)$$

$$\frac{\partial\left((1-\phi)\rho[SOM_2]\right)}{\partial t} = \frac{\partial\{(1-\phi)\rho D_B \frac{\partial[SOM_2]}{\partial x}\}}{\partial x} - \frac{\partial\{(1-\phi)\rho\omega[SOM_2]\}}{\partial x} - (1-\phi)\rho k_2[SOM_2] \quad (7)$$

$$\frac{\partial[SOM_3]}{\partial t} = 0 \quad \text{and} \quad \frac{\partial[SOM_3]}{\partial x} = 0, \quad (8)$$

where D_B (cm^2 yr^{-1}) is the bioturbation coefficient, ω (cm yr^{-1}) is the sedimentation rate, x (cm) is sediment depth, t (yr) is time, ϕ is sediment porosity, ρ is density of the sediment solid phase (2.5 g cm^{-3}), k_1 and k_2 are the rate constants for degradation of SOM_1 and SOM_2, respectively, and the brackets denote concentration.

Compaction is simulated by decreasing porosity exponentially with depth:

$$\phi = (\phi_0 - \phi_\infty)\exp(-\beta x) + \phi_\infty \quad , \quad (9)$$

where ϕ_0 is the porosity at sediment-water interface, ϕ_∞ is porosity at infinite depth, and β is the scale-length coefficient. Values for porosity parameters (ϕ_0, ϕ_∞, β) are derived by fitting eq. (9) to measured porosity-depth distributions. Porosity in the water column is set to 1. An error function (erf) is used to maintain porosity continuity between the sediment and water column. The decrease in sedimentation rate with depth, due to compaction, is given by:

$$\omega = \omega_\infty \cdot \frac{(1-\phi_\infty)}{(1-\phi)}, \quad (10)$$

where the subscript (∞) denotes values at infinite sediment depth.

Depth-dependence of the mixing coefficient (D_B) is described by the complementary error function (erfc) (Robbins 1986):

$$D_B = \frac{D_{B0}}{2} erfc\left(\frac{x - X_{ML}}{\sigma}\right) \quad , \quad (11)$$

where D_{B0} is the bioturbation coefficient at sediment-water interface, X_{ML} is the depth where $D_B / D_{B0} = 0.5$, and σ is a constant that controls dD_B/dx in the vicinity of $x = X_{ML}$. Setting $\sigma = 2$ results in a relatively rapid decline in D_B at the base of the mixed layer. This model is a continuous equivalent of the traditional, simple two-layer mixing model that allows D_B to decrease continuously through the bottom of the mixed layer. The continuity of D_B is necessary for the stability of the numerical solution, and is also reasonable because one can envision that

bioturbation would not stop suddenly at a certain depth, but would decrease continuously with depth.

Equations (6), (7) and (8) assume that organic matter degradation rates are independent of the oxidant (oxygen, nitrate, sulfate, etc.). This assumption is widely used in diagenetic models (e.g., Dhakar and Burdige 1996; Soetaert et al. 1996a).

Our model assumes that aerobic respiration, nitrate reduction, sulfate reduction, and methane production are the dominant SOM decomposition pathways (organic matter oxidation via Fe and/or Mn oxides are assumed to be less important). Many studies have shown that the oxidant (electron acceptor) that provides the greatest free energy yield during organic matter decomposition is used ahead of less energetic oxidants (Bender et al. 1977; Froelich et al. 1979; Emerson et al. 1980). Oxygen is the most favorable electron acceptor, followed by nitrate, and then sulfate. Fermentation, leading to methane production, generally occurs only after sulfate is depleted.

Error functions (and their complement) are used to simulate the sequential ordering of the organic matter decomposition reactions. Complementary error functions (f_1 , f_2 and f_3) approach one when oxygen, nitrate and sulfate concentrations are less than limiting values for microbial uptake (O^*, N^*, and S^*, respectively), and approach zero at higher values:

$$f_1 = 0.5 \cdot \mathrm{erfc}\left(\frac{[O_2] - O^*}{\sigma_O}\right) \approx \begin{cases} 1 & \text{if } [O_2] < O^* \\ 0 & \text{if } [O_2] > O^* \end{cases}, \tag{12}$$

$$f_2 = 0.5 \cdot \mathrm{erfc}\left(\frac{[NO_3^-] - N^*}{\sigma_N}\right) \approx \begin{cases} 1 & \text{if } [NO_3^-] < N^* \\ 0 & \text{if } [NO_3^-] > N^* \end{cases}, . \tag{13}$$

$$f_3 = 0.5 \cdot \mathrm{erfc}\left(\frac{[SO_4^{2-}] - S^*}{\sigma_S}\right) \approx \begin{cases} 1 & \text{if } [SO_4^{2-}] < S^* \\ 0 & \text{if } [SO_4^{2-}] > S^* \end{cases}. \tag{14}$$

Thus, f_1 can be used to inhibit denitrification, sulfate reduction, and fermentation if oxygen concentrations are not limiting to aerobic bacteria. Likewise, the functions (1- f_1), (1- f_2) and (1- f_3) serve to simulate the first-order dependence of respiration rates on oxidant concentrations as electron acceptors approach threshold levels.

These inhibition functions offer several advantageous over the more commonly used Michaelis-Menten equation (e.g., Devol 1978; Rabouille and Gaillard 1991; Boudreau 1996; Dhakar and Burdige 1996): (1) they provide a better fit to published oxygen uptake rate versus oxygen concentration data (Devol 1978); (2) they provide mathematical simplicity and computational efficiency; and (3) they assure electron balance by quantitatively linking organic matter decomposition and oxidant consumption.

Limiting concentrations for oxidants used in the model are as follows: 2 μM for oxygen, 2 μM for nitrate, and 0.2 mM for sulfate (Billen 1978; Metcalf and Eddy 1979; Esteves et al. 1986; Murry et al. 1989; Nielsen et al. 1990; Van Cappellen et al. 1993; Van Cappellen and Wang

1995; Soetaert et al. 1996a). The gradient parameters (σ_O , σ_N , and σ_S) are set at 0.5 times the limiting concentration.

The general diagenetic equation for oxygen includes terms for molecular diffusion, bioturbation, eddy diffusion, advection, and oxygen consumption:

$$\begin{aligned}\frac{\partial(\phi[O_2])}{\partial t} = & \frac{\partial\{\phi(D_B + D_S^{O_2} + D_E)\frac{\partial[O_2]}{\partial x}\}}{\partial x} - \frac{\partial(\phi\upsilon[O_2])}{\partial x} \\ & -\phi(1-f_1)\{R_1k_1[SOM_1] + R_1k_2[SOM_2] + 2k_N[NH_4^+] + 2k_{Mo}[CH_4]\} \\ & -\phi k_{ODU1}[ODU_1][O_2] - \phi k_{ODU2}[ODU_2][O_2]\end{aligned} \quad (15)$$

where υ (cm yr^{-1}) is pore water burial velocity. The relationship between ω and υ is:

$$-\frac{\partial(\phi\upsilon)}{\partial x} = \frac{\partial[(1-\phi)\omega]}{\partial x}. \quad (16)$$

$D_S^{O_2}$ is the sediment diffusion coefficient for oxygen calculated from the molecular diffusion coefficient (D_0) and corrected for tortuosity (Ullman and Aller 1982):

$$D_S = \phi^2 D_0. \quad (17)$$

R_1 is a stoichiometric coefficient that relates organic matter oxidation and oxygen consumption. We assume that SOM has an oxidation state similar to carbohydrate so that one carbon is degraded for each oxygen molecule (i.e., R_1 equals 1). k_N and k_{Mo} are rate constants for nitrification and aerobic methane oxidation, respectively. As described above, the term (1 - f_1) serves to simulate the cessation of aerobic processes when oxygen concentrations drop below the limiting value. *ODU* denotes oxygen-demanding units, which includes all the direct and indirect byproducts of sulfate reduction that could potentially consume oxygen (i.e., FeS, Fe_2S, S^{2-}, Fe^{2+}). ODU_1 represents soluble reduced compounds that are subject to molecular diffusion, while ODU_2 represents compounds associated with the solid phase that are transported by sedimentation and bioturbation. k_{ODU1} and k_{ODU2} are oxidation rate constants of ODU_1 and ODU_2, respectively.

A similar diagenetic equation is used to describe nitrate concentration:

$$\begin{aligned}\frac{\partial(\phi[NO_3^-])}{\partial t} = & \frac{\partial\{\phi(D_B + D_S^{NO_3^-} + D_E)\frac{\partial[NO_3^-]}{\partial x}\}}{\partial x} - \frac{\partial(\phi\upsilon[NO_3^-])}{\partial x} \\ & +\phi(1-f_1)(k_N[NH_4^+]) - \phi f_1(1-f_2)\{R_2k_1[SOM_1] + R_2k_2[SOM_2]\}\end{aligned}, \quad (18)$$

where $D_S^{NO_3^-}$ is the diffusion coefficient for nitrate; R_2 is a stoichiometric coefficient that relates organic matter oxidation and nitrate consumption (i.e., R_2 equals 4/5), and (1- f_2) is the limitation

function that makes denitrification only occur in the presence of nitrate. Coupling f_1 and f_2 in eq. (18) assures that denitrification is limited by nitrate and is inhibited by oxygen.

The diagenetic equation for total ammonium is:

$$\begin{aligned}\frac{\partial(\phi[NH_4^+])}{\partial t} = & \frac{\partial\{\frac{K_{ad}D_B}{1+K_{ad}}\cdot\frac{\partial(\phi[NH_4^+])}{\partial x}+\frac{\phi(D_B+D_S^{NH_4^+}+D_E)}{1+K_{ad}}\cdot\frac{\partial[NH_4^+]}{\partial x}\}}{\partial x} \\ & -\frac{1}{1+K_{ad}}\frac{\partial(\phi\upsilon[NH_4^+])}{\partial x}-\frac{K_{ad}}{1+K_{ad}}\frac{\partial(\phi\omega[NH_4^+])}{\partial x} \\ & +\phi R_3\{k_1[SOM_1]+k_2[SOM_2]\}-\phi(1-f_1)(k_N[NH_4^+])\end{aligned} \quad (19)$$

where $D_S^{NH_4^+}$ is the diffusion coefficient for ammonium, R_3 is a stoichiometric coefficient dependent on the C:N ratio of the degradable sedimentary organic matter (i.e., R_3 equals N:C ratio), and K_{ad} is the dimensionless adsorption coefficient for ammonium calculated from the distribution coefficient of ammonium between solid matter and pore water (K_D (mL g^{-1})):

$$K_{ad} = K_D\rho\frac{1-\phi_\infty}{\phi_\infty}. \quad (20)$$

We assume that K_{ad} is constant and independent of depth (Boudreau 1996, Van Cappellen and Wang 1996). Total ammonium produced in bulk sediment must be corrected for adsorption in order to calculate the ammonium concentration in the pore water.

The diagenetic equation for sulfate is:

$$\begin{aligned}\frac{\partial(\phi[SO_4^{2-}])}{\partial t} = & \frac{\partial\{\phi(D_B+D_S^{SO_4^{2-}}+D_E)\frac{\partial[SO_4^{2-}]}{\partial x}\}}{\partial x}-\frac{\partial(\phi\upsilon[SO_4^{2-}])}{\partial x} \\ & -\phi f_1 f_2(1-f_3)\{R_3k_1[SOM_1]+R_3k_2[SOM_2]+k_{Ma}[CH_4]\}\end{aligned}, \quad (21)$$

where $D_S^{SO_4^{2-}}$ is the diffusion coefficient for sulfate, R_3 is a stoichiometric coefficient that relates organic matter oxidation and sulfate consumption (i.e., R_3 equals ½), the term $f_1f_2(1-f_3)$ assures that sulfate reduction occurs only occur when oxygen and nitrate are used up and sulfate is abundant, and k_{M_a} is the rate constant for anaerobic methane oxidation.

The diagenetic equation for methane is:

$$\frac{\partial(\phi[CH_4])}{\partial t} = \frac{\partial\{\phi(D_B + D_S^{CH_4} + D_E)\frac{\partial[CH_4]}{\partial x}\}}{\partial x} - \frac{\partial(\phi\upsilon[CH_4])}{\partial x} + \phi f_1 f_2 f_3(1-f_4)\{R_4 k_1[SOM_1] + R_4 k_2[SOM_2]\} - \phi(1-f_1)k_{Mo}[CH_4] - \phi f_1 f_2(1-f_3)k_{Ma}[CH_4] \quad , \qquad (22)$$

where $D_S^{CH_4}$ is the diffusion coefficient for methane, R_4 is a stoichiometric coefficient that relates organic matter oxidation and methane production (i.e., R_3 equals ½). The term 1- f_4 partitions methane into a gas phase when the porewater methane concentration exceeds in situ saturation.

The diagenetic equation for total dissolved CO_2 (ΣCO_2) is:

$$\frac{\partial(\phi[\Sigma CO_2])}{\partial t} = \frac{\partial\{\phi(D_B + D_S^{CO_2} + D_E)\frac{\partial[\Sigma CO_2]}{\partial x}\}}{\partial x} - \frac{\partial(\phi\upsilon[\Sigma CO_2])}{\partial x} + \phi\{k_1[SOM_1] + k_2[SOM_2]\}. \qquad (23)$$

The diagenetic equation for ODU_1 (dissolved oxygen demand) is:

$$\frac{\partial(\phi[ODU_1])}{\partial t} = \frac{\partial\{\phi(D_B + D_S^{ODU1} + D_E)\frac{\partial[ODU_1]}{\partial x}\}}{\partial x} - \frac{\partial(\phi\upsilon[ODU_1])}{\partial x} + \phi f_{ODU1} f_1 f_2(1-f_3)\{R_3 k_1[SOM_1] + R_3 k_2[SOM_2]\} - (1-f_1)k_{ODU1}[O_2][ODU_1] \qquad (24)$$

The molecular diffusion coefficient of Fe^{2+} is used as D_S^{ODU1}, k_{ODU1} is the rate constant for ODU_1 oxidation (taken as the rate constant of Fe^{2+} oxidation; Fossing e al. 2004), f_{ODU1} is the fraction of ODU_1 among the total ODU produced through sulfate reduction.

The diagenetic equation for ODU_2 (particulate oxygen demand) is:

$$\frac{\partial((1-\phi)\rho[ODU2])}{\partial t} = \frac{\partial\{(1-\phi)\rho D_B\frac{\partial[ODU2]}{\partial x}\}}{\partial x} - \frac{\partial((1-\phi)\rho\omega[ODU2])}{\partial x} + (1-\phi)\rho(1-f_{ODU1})f_1 f_2(1-f_3)\{R_3 k_1[SOM_1] + R_3 k_2[SOM_2]\} - (1-\phi)\rho(1-f_1)k_{ODU2}[O_2][ODU2] \quad , \qquad (25)$$

where k_{ODU2} is the rate constant of ODU_2 oxidation (taken as the rate constant for FeS oxidation is used as k_{ODU2}; Fossing et al. 2004).

BOUNDARY CONDITIONS

The upper boundary is set 1-cm above sediment surface and the lower boundary is at 100-cm depth in the sediment. The spatial resolution of the model is depth-dependent; highest from –1 to 1 cm to catch the detail of aerobic and denitrification zones. SOM pools have flux conditions at the upper boundary. Concentrations of oxygen, ammonium, and nitrate at the upper boundary are used as upper boundary conditions. Bottom water concentrations of sulfate and ΣCO_2 are calculated from salinity. Methane, ODU_1, and ODU_2 are set to zero concentration at the upper boundary. For all the species, the lower boundary conditions are set to zero concentration gradient.

MODEL CALIBRATION

Many parameters in the sediment model are directly or indirectly determined from data collected at ModMon station MM70 (Figure 1). MM70 is located in the middle of the Neuse Estuary and sediment at this site is more organic-rich relative to other areas in the estuary. We use this station as our test site because it is located in a region of the estuary that is most subject to hypoxia, algal blooms, and fish kills.

The measured parameters include: sedimentation rate, bioturbation coefficient, bioturbation depth, porosity, C:N ratio of *SOM* in the upper 3 cm of sediment, and ammonium adsorption coefficient. For example, sedimentation rate and bioturbation coefficient have been determined using geochronological tracers (^{210}Pb and ^{137}Cs), the C:N ratio of the degradable organic matter in the upper 3 cm of sediment has been estimated from ammonium and ΣCO_2 production rate experiments, and ammonium adsorption coefficients have been determined by potassium displacement studies. Model parameters that have not been measured are calibrated by fitting the model-generated concentration and reaction rate profiles with measured data in order to optimize the values of the parameters. Adjustable parameters include: (1) fluxes of SOM_1 and SOM_2 to the sediment; (2) degradation rate constants for SOM_1 and SOM_2 (k_1 and k_2, respectively); (3) nitrification rate constant (k_N); (4) rate constants for aerobic and anaerobic methane oxidation (k_{Mo} and k_{M_a}); (5) C:N ratio of the SOM_2; and (6) fraction of ODU_1 among total ODU.

The sediment model is run to a quasi-steady state by allowing bottom water temperature, salinity, oxygen, nitrate, and ammonium to vary seasonally without inter-annual variability. At quasi-steady-state, model-generated concentration profiles for any species vary from month to month, but are consistent from year-to-year. Adjustable parameters in the sediment model are tuned as follows: the depositional flux and rate constant for SOM_2 are constrained by measured ΣCO_2, sulfate, and methane profiles and denitrification rate measurements; the depositional flux and rate constant for SOM_1 is determined by oxygen concentration profile measured by microelectrode; the rate constant for nitrification (k_N) is constrained by the measured benthic ammonium flux; rate constants for aerobic and anaerobic methane oxidation (k_{Mo} and k_{M_a}) are constrained by the measured methane profiles; the C:N ratio of *SOM* below 3 cm sediment depth is constrained by ammonium and ΣCO_2 profiles, the fraction of ODU_1 among total ODU is constrained by Fe^{2+} and S^{2-} concentrations that are typical of estuarine sediments.

Results of the calibrated model for sediment from MM70 are shown in Figure 2, and the calibrated model parameters are summarized in Table 1.

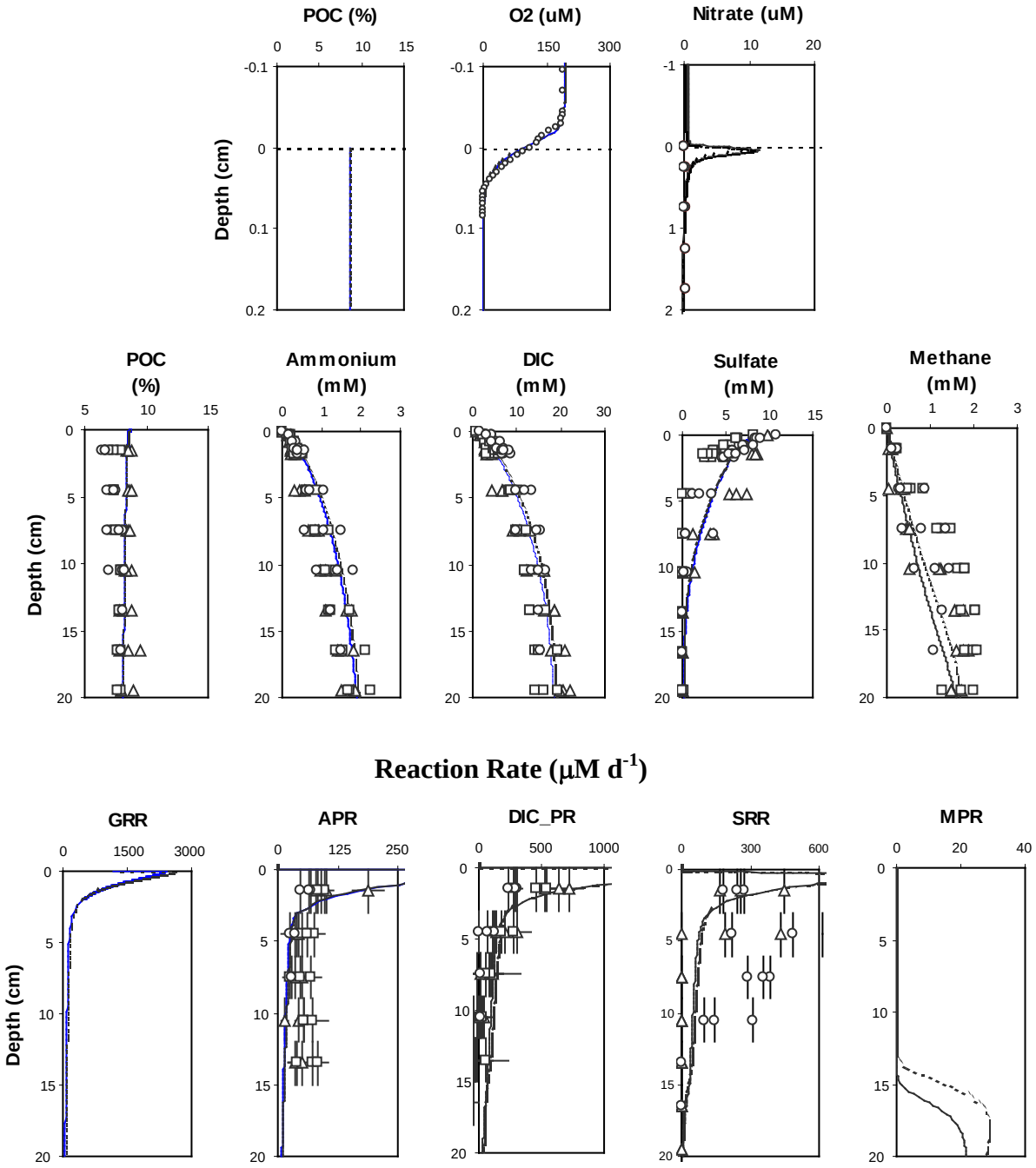

Figure 2. Model fit for sediment from station MM70: particulate organic carbon (POC), oxygen, nitrate, ammonium, dissolved inorganic carbon (DIC), sulfate and methane profiles; remineralization rate (GRR), ammonium production rate (APR), DIC production rate (DIC_PR), sulfate reduction rate (SRR), and methane production rate (MPR) profiles. Open circles, squares and triangles are data from different sampling times (in June and July). The solid and dotted curves are model predicted profiles for month of June and July, respectively.

Table 1. Calibrated model parameters and parameters used in the simulations.

Model parameters	Calibrated parameters	POC reduction	Anoxia	Current velocity test
ϕ_0	0.96783	0.96783	0.96783	0.96783
ϕ_∞	0.89735	0.89735	0.89735	0.89735
β (cm^{-1})	0.75696	0.75696	0.75696	0.75696
D_{B0} ($cm^2\ yr^{-1}$)	60	60	60	60
X_{ML} (cm)	28	28	28	28
ω_∞ ($g\ cm^{-2}\ yr^{-1}$)	0.2	0.2	0.2	0.2
SOM1 flux ($mmol\ m^{-2}\ d^{-1}$)	24.8	Variable	24.8	24.8
SOM2 flux ($mmol\ m^{-2}\ d^{-1}$)	13.3	Variable	13.3	13.3
SOM3 flux ($mmol\ m^{-2}\ d^{-1}$)	36.5	36.5	36.5	36.5
k_1 (yr^{-1})	100	100	100	100
k_2 (yr^{-1})	0.6	0.6	0.6	0.6
C/N above 3 cm	4.5	4.5	4.5	4.5
C/N below 3 cm	6	6	6	6
K_{ad} ($mL\ g^{-1}$)	8	8	8	8
K_N (yr^{-1})	80000	80000	80000	80000
K_{M_o} (yr^{-1})	10^6	10^6	10^6	10^6
K_{M_a} (yr^{-1})	0	0	0	0
T (ºC)	Varies monthly	18	27.6	25.6
U_{100} ($cm\ s^{-1}$)	5	5	5	Variable
Salinity (psu)	10	10	10	10
Water depth (m)	3.5	3.5	3.5	3.5
Benthic oxygen (μM)	Varies monthly	284	Variable	192.8; 62.5; 0
Benthic nitrate (μM)	Varies monthly	2.7	0.1	0.56
Benthic ammonium (μM)	Varies monthly	6.75	1.25	2.21

MODEL RESULTS AND DISCUSSION

Output from the sediment model includes: benthic fluxes of oxygen, nitrate, and ammonium, concentration profiles of all chemical species, and depth distributions of oxygen consumption rate, nitrification rate, denitrification rate, and organic matter degradation rates. Here, we use the sediment model to evaluate how sediment pools and processes respond to (1) reduced nitrogen loading, (2) sudden changes in bottom water oxygen concentration, and (3) variable bottom currents. For all applications, the quasi-steady state provides the initial conditions, and the model parameters used in each simulation are summarized in Table 1.

IMPACT OF REDUCED NITROGEN LOADING ON BENTHIC FLUXES

We assume that reduced nitrogen loading will translate into lower productivity in the estuary and less reactive SOM deposition to the sediment. Here, we conduct a sensitivity analysis to see how sediments respond to four SOM-flux reduction scenarios: 10%, 20%, 30% and 40% reduction of reactive SOM (i.e., SOM_1 + SOM_2). For each scenario, we consider two flux reduction patterns: instantaneous SOM flux reduction and gradual SOM flux reduction during a ten-year period. The year-round average bottom water temperature, benthic oxygen, nitrate, and ammonium concentrations are used in the simulation.

Results of the simulation are shown in Figure 3. Instantaneous reduction of SOM deposition results in a relatively gradual reduction in the benthic oxygen flux. The relatively slow response time of the sediment oxygen demand to reduced SOM deposition (ca. 10 years) is due to the large repository of organic matter contained in the sediment. In contrast, denitrification and benthic ammonium flux both decrease rapidly in response to a sudden reduction in SOM deposition. Within 10-15 years after the start of the SOM flux reduction, benthic fluxes and denitrification rates are similar for instantaneous and gradual reduction scenarios. It takes the sediment column approximately 45 years to reach a new steady-state following a sudden or gradual reduction in SOM deposition.

Sediment oxygen demand decreases 5%, 11%, 20%, and 30% in response to SOM flux reductions of 10%, 20%, 30% and 40%, respectively. Though SOM deposition is the ultimate source of sediment oxygen demand, the benthic oxygen flux does not decrease linearly with SOM deposition. This is because reduced SOM flux results in deeper oxygen penetration allowing a more efficient oxidation of the upward diffusive flux of reduced solutes such as ammonium, sulfide, and ferrous iron.

Denitrification decreases 3%, 6%, 10%, and 15% for the four SOM reduction scenarios, respectively. The modest reduction in denitrification is related to two competing factors. On the one hand, reduced SOM input decreases denitrification by allowing a greater fraction of the organic matter decomposition to proceed via aerobic respiration. On the other hand, reduced SOM input allows for enhanced nitrification which stimulates denitrification by providing additional nitrate. Thus, the net denitrification rate decrease is not as significant as SOM reduction.

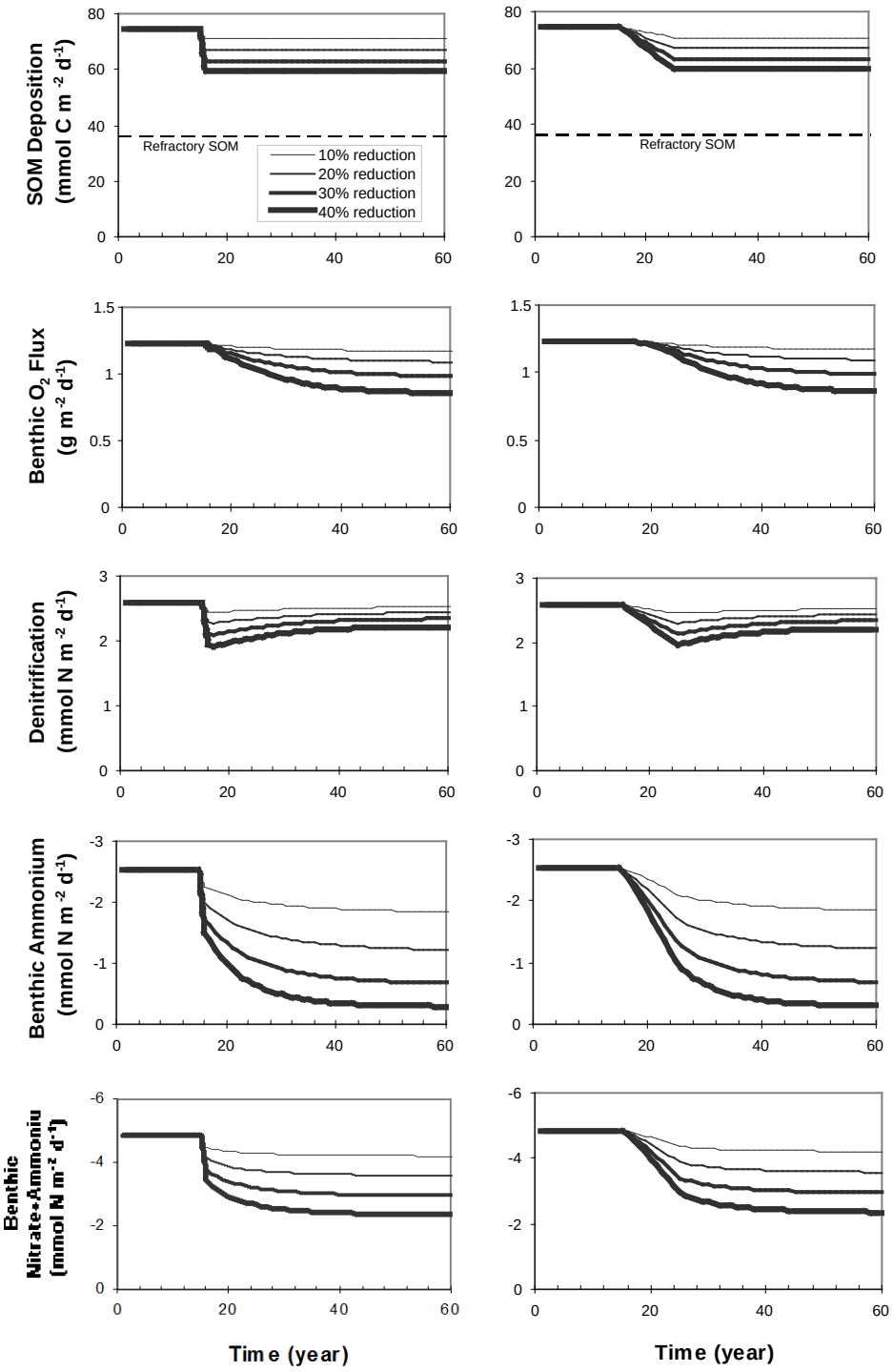

Figure 3. Modeling results for simulating POC flux reduction.

The benthic ammonium flux also shows a nonlinear response to decreased SOM input. However, in this case the feedback in positive. The flux of ammonium from the sediments decreases by 27%, 52%, 73% and 88% in response to 10%, 20%, 30% and 40% reductions in SOM deposition, respectively. As discussed above, reduced SOM translates to deeper oxygen penetration and more effective nitrification.

The net result of 10%, 20%, 30%, and 40% reductions in SOM influx is to reduce the total benthic flux of reactive nitrogen by 13%, 26%, 39%, and 52%, respectively. The excess nitrogen removal is due to enhanced denitrification associated with stimulated nitrification resulting from deeper oxygen penetration.

In addition, there may be positive feedbacks resulting from sediment-water column coupling. Given that the benthic ammonium flux is equivalent to about 25% of the annually averaged nitrogen demand of primary producers (Alperin et al. 2000), we expect reduced primary production and hence SOM deposition due to decreases in the benthic flux of reactive nitrogen. Furthermore, the ratio of ammonium:nitrate in the benthic flux decreases dramatically as a result of reduced SOM deposition. This shift will result in lower rates of water column nitrification, and possibly reduced oxygen demand in the bottom water.

IMPACT OF BOTTOM WATER HYPOXIA ON BENTHIC FLUXES

During the summer months, bottom water oxygen concentrations in the Neuse River estuary are highly variable in time, shifting from oxic to hypoxic or anoxic over periods of hours. In this experiment, we simulate the sediment response to a sudden period of bottom water anoxia that persists for two weeks. Bottom water temperature, benthic oxygen, nitrate and ammonium concentrations for month of July are used in this simulation.

Model results are summarized in Figure 4. Aerobic respiration, nitrification, and denitrification are restricted to the upper ~1 mm of the sediment column during the summer months. Molecular diffusion is quite fast over these space scales (ca. 10 min), so that benthic fluxes of oxygen, ammonium, and nitrate respond quickly to changes in bottom water oxygen. The benthic oxygen flux decreases in proportion to the oxygen concentration above the sediment-water interface. Oxygen depletion in the bottom water inhibits nitrification causing denitrification to nearly shut down (very little denitrification is supported by nitrate in the overlying water).

During the period of anoxia, the ammonium flux to overlying water increases three-fold while the flux of nitrate to the overlying water is reduced to nearly zero. The net effect of anoxia is a 30% increase in the benthic flux of reactive nitrogen to the water column. This represents another potential positive feedback: reduced nitrogen loading to the estuary reduces estuarine production and SOM deposition, which reduces sediment and water column oxygen demand, which reduces the frequency and duration of bottom water hypoxia, which results in a decrease in the benthic flux of reactive nitrogen to the water column, which further represses estuarine production.

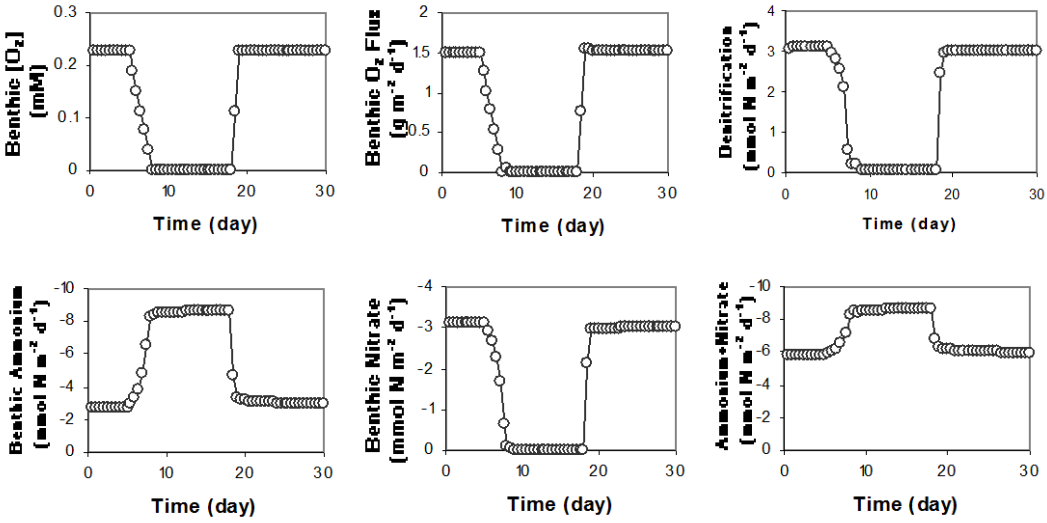

Figure 4. Modeling results for simulating anoxic condition.

IMPACT OF BOTTOM CURRENT ON BENTHIC FLUXES

Current velocity in the bottom water (1-meter above bottom) is highly variable throughout the estuary (e.g., Figure 5, Luettich et al. unpublished data). Bottom current controls the thickness of the diffusive boundary layer and hence has an impact on sediment-water exchange and benthic processes. The sensitivity of the sediment system to bottom current introduces internal variability that must be resolved in order to discern trends associated with reductions in nitrogen loading and SOM deposition. Here, we test the sensitivity of the sediment system to bottom current for three periods, each lasting 25 hours:

Case 1: a period of relatively low velocity and low variability;
Case 2: a period of high average velocity and high variability;
Case 3: a period of moderate velocity and variability.

Since the currently velocity data are measured in June, bottom water temperature, benthic oxygen, nitrate and ammonium concentrations in the month of June are used in this simulation.

Average oxygen penetration depth and benthic oxygen flux change dramatically in response to changes in bottom water velocity. However, the sediment response to bottom current is not linear. The average current velocity in Case 2 is almost three times that in Case 1, while oxygen penetration depth and oxygen consumption rate in Case 2 are only about two times that in Case 1. This is because oxygen penetration depth is controlled by the thickness of the diffusive boundary layer, and the thickness of the diffusive boundary layer is most sensitive to current velocity when the velocity is low. Case 2 has the highest average current velocity, highest oxygen penetration depth, oxygen consumption rate and nitrate flux. The average nitrate flux out of the sediment is higher in Case 2 because of the higher nitrate concentration in sediment due to increased nitrification when oxygen penetrates deeper. Denitrification is lowest in Case 2: with

higher current velocity, oxygen penetrates deeper, forcing denitrification to greater depth. The benthic ammonium flux is nearly unchanged with current velocity.

Figure 6 shows how benthic fluxes and sediment processes respond to changes in current velocity. In general, oxygen penetration depth and benthic fluxes of oxygen and nitrate track bottom current velocity, while the denitrification rate and ammonium flux are relatively insensitive to bottom current velocity.

The combined effects of bottom water oxygen concentrations and changing bottom currents are simulated for Case 1. Three bottom water oxygen scenarios are tested: 80% oxygen saturation (192.8 μM), threshold of hypoxia (62.5 μM), and anoxia. The modeling results are shown in Figure 7. The sensitivity of the sediments decreases at lower bottom water oxygen concentrations.

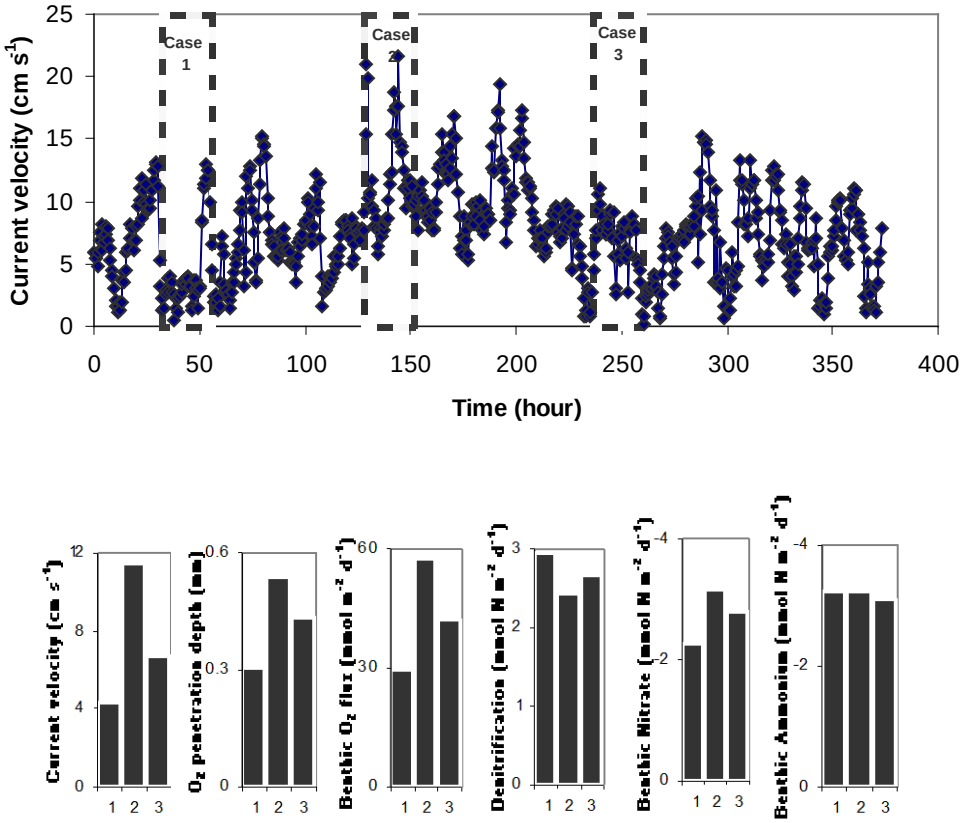

Figure 5. Current velocity variation case study I: three current velocity cases and model predicted average reaction rates and fluxes at each case. Shows current velocity measured every half an hour from a station in upper Neuse Estuary in late June, 2003 (Rick Luettich, unpublished data).

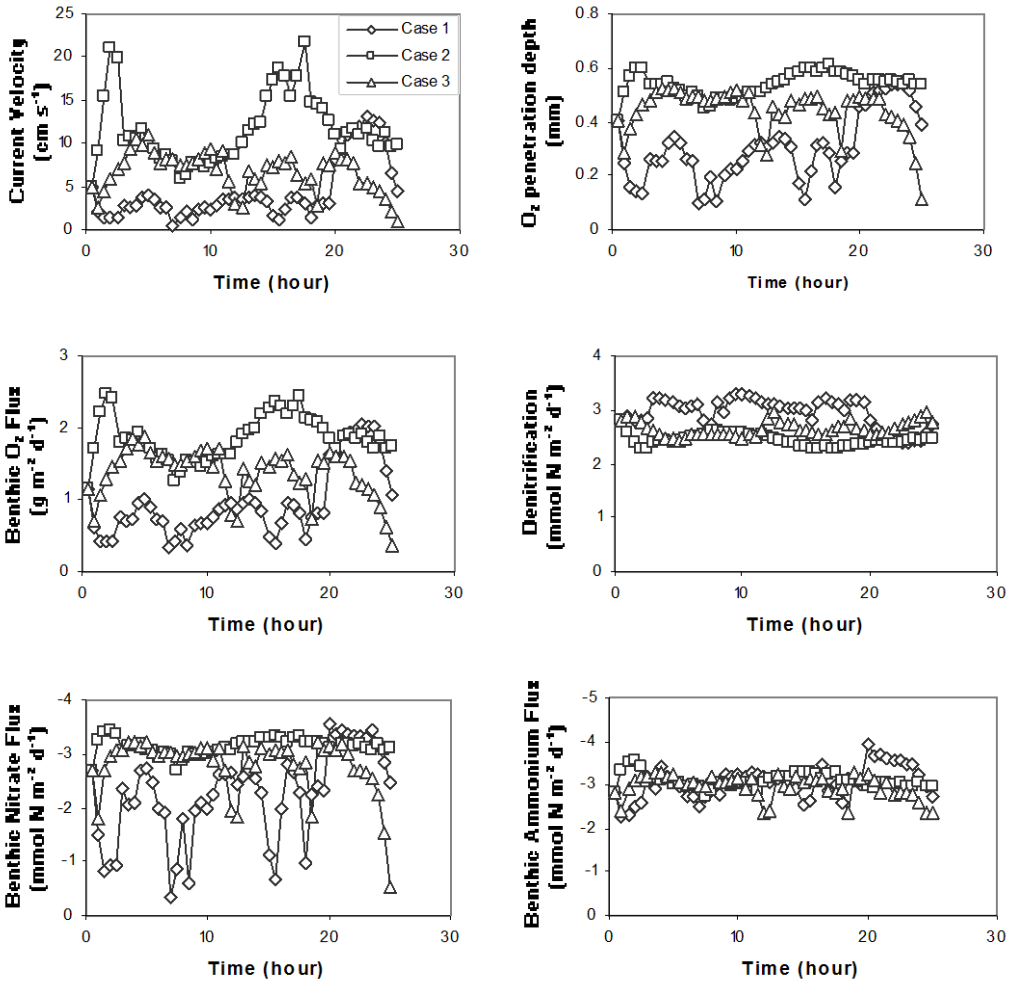

Figure 6. Current velocity variation case study II: reaction rates and fluxes versus time in the three cases.

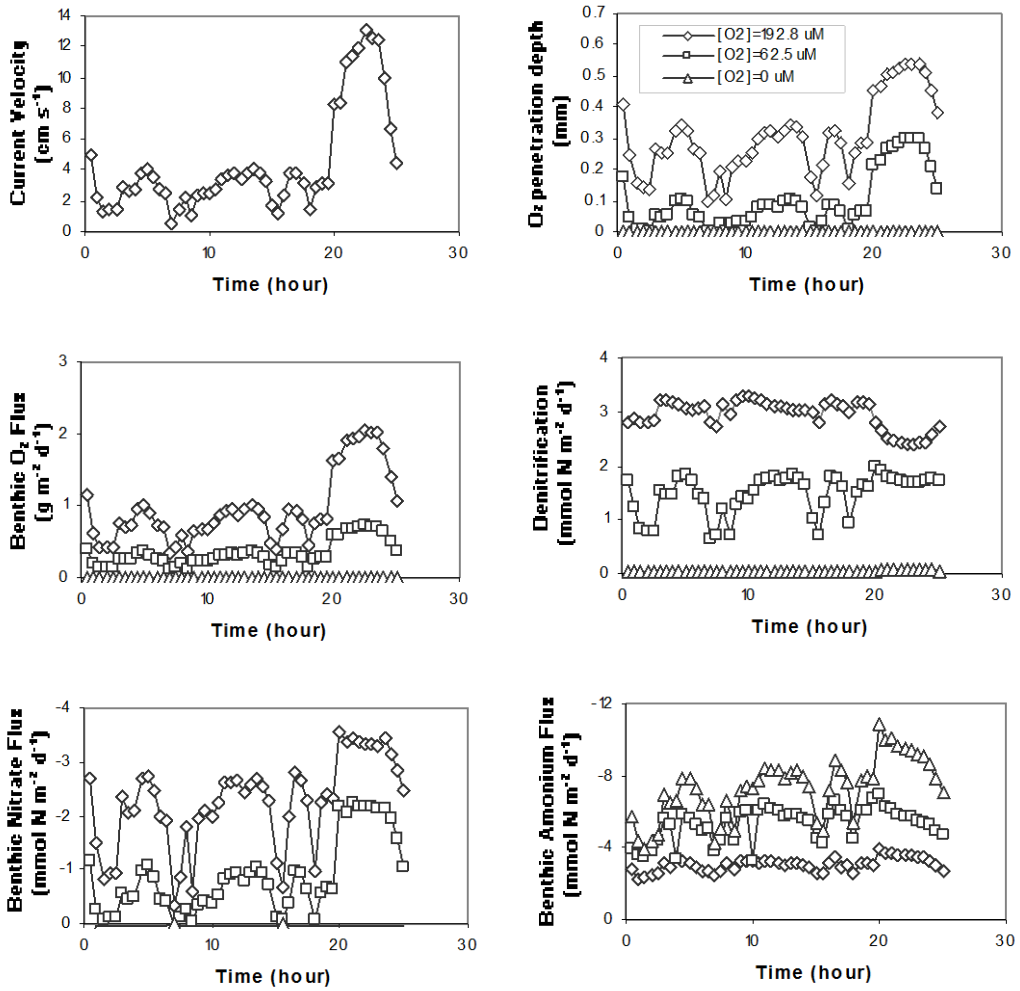

Figure 7. Current velocity variation case study III: reaction rates and fluxes versus time at three different bottom water oxygen concentrations, i.e., 80% oxygen saturation, hypoxia threshold value (62.5 μM), and zero oxygen concentration.

CONCLUSIONS

Sediment-water column interactions in the Neuse River estuary are highly nonlinear and characterized by numerous positive and negative feedbacks between master variables (such as nitrogen loading and sediment organic matter deposition) and response variables (such as internal cycling of nitrogen and total oxygen demand). The sediment diagenesis model presented here is a tool for making quantitative predictions of how the sediment system, and resulting benthic fluxes, respond to various scenarios involving changes in the master variables. The most important results from the sediment model are as follows:

4. Sediment oxygen demand responds slowly to a sudden reduction sedimentary organic matter deposition. This is because the sediments contain a large repository of reactive organic that serves as a time-release source of oxygen demand. Following a reduction of organic matter deposition, it will take 15 years for the sediment oxygen demand to decrease to 50% of its steady-state value.

5. The reduction in the steady-state benthic oxygen flux is not proportionate to the reduction in SOM deposition. For example, a 30% reduction in SOM flux translates to only a 20% reduction in benthic oxygen flux.

6. The reduction in the steady-state benthic ammonium flux is more than proportionate to the reduction in SOM deposition. For example, a 30% reduction in SOM flux translates to a 73% reduction in benthic ammonium flux.

7. Reduced SOM deposition will shift the nitrogen species released from the sediments in favor of more nitrate and less ammonium.

8. Episodic hypoxia and anoxia in the bottom water result in elevated benthic fluxes of reactive nitrogen to the water column.

9. Variations in bottom current introduce internal variability in sediment-water column exchange processes. The benthic oxygen flux increases markedly with bottom current while denitrification slightly reduced at higher bottom water velocities. The benthic ammonium flux is controlled by processes well below the diffusive boundary layer and is little affected by bottom current.

REFERENCE LIST

Alperin, M. J., E. J. Clesceri, J. T. Wells, D. B. Albert, J. E. McNinch, and C. S. Martens. 2000. Sedimentary processes and benthic-pelagic coupling. In: *Neuse River Estuary Modeling and Monitoring Project: Final Report—Monitoring Phase*, R. A. Luettich, Jr. (Editor), Water Resources Research Institute Report, 63-105.

Bender, M. L., K. A. Fanning, P. N. Froelich, F. R. Heath, and V. Maynard. 1977. Interstitial nitrate profiles and oxidation of sedimentary organic matter in the eastern equatorial pacific. *Science* **198**:605-609.

Billen, G. 1978. A budget of nitrogen recycling in North Sea sediments off the Belgian coast. *Estuarine Coastal Mar. Sci.* **7**: 127-146.

Boudreau, B. P. 1996. A method-of-lines code for carbon and nutrient diagenesis in aquatic sediments. *Computers & Geosciences*. 22:479-496.

Boudreau, B. P. 1997. *Diagenetic Models and Their Inplementation.* Springer-Verlag, N. Y.

Christian, R. R., J. N. Boyer, D. W. Stanley, and W. M. Rizzo. 1992. Network analysis of nitrogen cycling in and estuary, p. 217-247. In C.J. Hurst(ed). *Modeling the Metabolic and Physiologic Activities of Microorganisms*, John Wiley and Sons, New York.

Devol, A. H. 1978. Bacterial oxygen uptake kinetics as related to biological processes in oxygen deficient zones of the oceans. *Deep-Sea Res.* **25**: 137-146.

Dhakar, S. P. and D. J. Burdige. 1996. A coupled, non-linear, steady state model for early diagenetic processes in pelagic sediment. *Am. J. Sci*. **296**: 296-330.

Dodd, R. C., P A. Cunningham, R. J. Curry, and S. J. Syichter. 1993. Watershed planning in the Albemarle-Pamlico Estuarine System, Report No. 93-01, Research Triangle Institute, Research Triangle Park, NC Department of Environment, Health, and Natural Resources.

Emerson, S., R. Jahnke, M. Bender, P. Froelich, P. Klinkhammer, C. Bowser, and G. Setlock. 1980. Early diagenesis in sediments from the eastern equatorial Pacific. I. Pore water nutrient and carbonate results. *Earth Planet. Sci. Lett.* **49**: 57-80.

Esteves, J. L., G. Mille, F. Blanc, and J. C. Bertrand. 1986. Nitrate reduction activity in a continuous flow-through system in marine sediments. *Microb. Ecol.* **12**: 283-290.

Fossing, H, Berg, P, Thamdrup, B, Rysgaard, S, Sørensen, H. M., and Nielsen, K. 2004. A model set-up for an oxygen and nutrient flux model for Aarhus Bay (Denmark). NERI Technical Report, No. 483. 65pp.

Froelich, P. N., G. P. Klinkhammer, M. L. Bender, N. L. Luedtke, G. R. Heath, D. Cullen, P. Dauphin, D. Hammond, B. Hariman, and V. Maynard. 1979. Early oxidation of organic

matter in pelagic sediments of the eastern equatorial Atlantic: suboxic diagenesis. *Geochim. Cosmochim. Acta.* **43**:1075-1090.

Harned, D. A. and M. S. Davenport. 1990. Water-quality trends and basin activities and characteristics for the Albemarle-Pamlico Estuarine System, NC and VA. Report 90-398, U.S. Geologic Survey, Raleigh, NC.

Harington, D. and D. Stotts. 2003. DeCo: A declarative coordination framework for scientific model federations. Technical Report TR03-017, Department of Computer Science, Univ. of North Carolina at Chapel Hill.

Hickey, B., E. Baker, and N. Kachel. 1986. Suspended particle movement in and around Quinault Submarine Canyon. *Mar. Geol.* **71**:35-83.

Jørgensen, B. B., M. Bang, and T. H. Blachburn. 1990. Anaerobic mineralization in marine sediments from the Baltic Sea-North Sea transition. *Mar. Ecol. Progr. Ser.* **59**: 39-54.

Kemp, W. M., P. Sampie, J. Caffrey, M. Mayer, K. Henriksen, and W. R. Boynton. 1990. Ammonium recycling versus denitrification in Chesapeake Bay sediments. *Limnol. Oceanogr.* **35**:1545-1563.

Metcalf and Eddy Inc. 1979. Theoretical model for manganese distribution in calcareous sediment cores. *J. Geophys. Res.* **76**: 2179-2186.

Murry, R. E., L. L. Parson, and M. S. Smith. 1989. Kinetics of nitrate utilization by mixed populations of denitrifying bacteria. *Appl. Environ. Microbiol.* **55**: 717-721.

Nielsen, L. P., P. B. Christensen, N. P. Revsbech, and J. Sørensen. 1990. Denitrification and oxygen respiration in biofilms studied with a microsensor for nitrous oxide and oxygen. *Microb. Ecol.* **19**: 63-72.

Nixon, S. W. 1981. Remineralization and nutrient cycling in coastal marine ecosystems. In: *Nutrients and Estuaries*, B.J. Nielson and L.E. Cronin (eds.), pp.111-138, Humana Press.

Opdyke, B. N., G. Gust, and J. R. Ledwell. 1987. Mass transfer from smooth alabaster surfaces in turbulent flows. *Geophys. Res. Lett.* **14**:1131-1134.

Paerl, H. W. 1987. Dynamics of blue-green algal blooms in the lower Neuse River, North Carolina: Causative factors and potential controls. Report No. 229. Water Resources Research Institute. University of North Carolina, Raleigh.

Paerl, H. W., M. A. Mallin, J. Rudek, and P. W. Bates. 1990. The potential for eutrophication and nuisance algal blooms in the lower Neuse River Estuary. Albemarle-Pamlico Estuarine Study Project No. 10-15. N. C. Dept. of Environmental, Health and Natural Resources, Raleigh, NC.

Rabouille, C. and J. –F. Gaillard. 1991. Towards the EDGE: Early diagenetic global explanation. A model depicting the early diagenesis of organic matter, O_2, NO_3, Mn, and PO_4. *Geochim. Cosmochim. Acta* **55**:2511-2525.

Robbins, J. A. 1986. A model for particle-selective transport of tracers in sediments with conveyor belt deposit feeders. *J. Geophys. Res.* **91**: 8542-8558.

Rudek, J., H. W. Paeral, M. A. Mallin, and P. W. Bates. 1991. Seasonal and hydrologic control of phytoplankton nutrient limitation in the lower Neuse River Estuary, North Carolina. *Mar. Ecol. Progr. Ser.* **75**:133-142.

Santschi, P. H., R. F. Anderson, M. Q. Fleisher, and W. Bowles. 1991. Measurements of diffusive sublayer thickness in the ocean by alabaster dissolution, and their implications for the measurements of benthic fluxes. *J. Geophys. Res.* **96**:10641-10657.

Soetaert, K., P. M. J. Herman, and J. J. Middelburg. 1996a. A model of early diagenetic processes from the shelf to abyssal depths. *Geochim. Cosmochim. Acta* **60**:1019-1040.

Soetaert, K., P. M. J. Herman, and J. J. Middelburg. 1996b. Dynamic response of deep-sea sediments to seasonal variations: a model. *Limnol. Oceanogr.* **41**: 1651-1668.

Sternberg, R. W. 1968. Friction factors in tidal channels with differing bed roughness. *Mar. Geol.* **6**:243-260.

Stow, C. A., M. E. Borsuk, and D. W. Stanley. 2001. Long-term changes in watershed nutrient inputs and riverine exports in the Neuse River, North Carolina. *Wat. Res.* **35**: 1489-1499.

Suess, R. 1980. Particulate organic carbon flux in the oceans: Surface productivity and oxygen utilization. *Nature,* 288:260-263.

Ullman, W. J. and R. C. Aller. 1982. Diffusion coefficients in near-shore marine sediments. *Limnol. Oceanogr.* **27**: 552-556.

Van Capppellen, P., J.-F. Gaillard, and C. Rabouille. 1993. Biogeochemical transformations in sediments: kinetic models of early diagenesis. *In* R. Wollast, F. T. Mackenzie and L. Chou [eds.], *Interactions of C, N, P and S Biogeochemical Cycles and Global Change*. Springer-Verlag. 401-445.

Van Cappellen, P, Wang, Y. 1996. Cycling of iron and manganese in surface sediments: a general theory for the coupled transport and reaction of carbon, oxygen, nitrogen, sulfur, iron and manganese. *Amer. J. Sci*. **296**:197-343.

Wang, Y., and P. Van Cappellen. 1996. A multicomponent reactive transport model of early diagenesis: application to redox cycling in coastal marine sediments. *Geochim. Cosmochim. Acta* **60**: 2993-3014.

Westrich, J. T., R. A. Berner. 1984. The role of sedimentary organic matter in bacterial sulfate reductionL the G model tested. *Limnol. Oceanogr*. **29**: 236-249.

APPENDIX

1. $CH_2O + O_2 \rightarrow CO_2 + H_2O$
2. $5CH_2O + 4NO_3 + 4H^+ \rightarrow 2N_2 + 5CO_2 + 7H_2O$
3. $2CH_2O + SO_4^{2-} + 2H^+ \rightarrow H_2S + 2CO_2 + 2H_2O$

   $H_2S \quad \cdots > \quad 2H^+ + ODU$
4. $2CH_2O \rightarrow CH_4 + CO_2$
5. $NH_4^+ + 2O_2 \rightarrow NO_3^- + H_2O + 2H^+$
6. $CH_4 + 2O_2 \rightarrow CO_2 + 2H_2O$
7. $CH_4 + SO_4^{2-} \rightarrow CO_2 + H_2S + 2OH^-$
8. $ODU + 2O_2 \rightarrow ODU \bullet O_4$